PERGAMON

Deep-Sea Research II 45 (1998) 2461–2487

DEEP-SEA RESEARCH
PART II

Upper ocean export of particulate organic carbon in the Arabian Sea derived from thorium-234

Ken Buesseler[a,*], Lary Ball[a], John Andrews[a], Claudia Benitez-Nelson[a], Rebecca Belastock[a], Fei Chai[b], Yi Chao[c]

[a] *Department of Marine Chemistry and Geochemistry, Woods Hole Oceanographic Institution, Woods Hole MA 02540, USA*
[b] *School of Marine Science, University of Maine, Orono ME 04469, USA*
[c] *Jet Propulsion Laboratory, California Institute of Technology, Pasadena CA 91109, USA*

Received 1 September 1997; received in revised form 25 May 1998; accepted 1 June 1998

Abstract

Thorium-234 is used in the Arabian Sea as a tracer of sinking particle fluxes. Samples were collected from January to August 1995 on four cruises during the Northeast Monsoon, the Spring Intermonsoon and the mid- and late-Southwest Monsoon periods. In this study, ^{234}Th activity distributions are used to quantify the ^{234}Th flux on sinking particles, and the measured ratio of particulate organic carbon (POC) to particulate ^{234}Th is used to convert from ^{234}Th to POC export at 100 m. The calculated POC fluxes range from < 1 to > 25 mmols C m^{-2} d^{-1}, and strong seasonal and spatial gradients are observed. The single largest feature is a basin-wide export maximum associated with the late-SW Monsoon cruise when POC export rates are 17–28% of the observed primary production rates along the southern sampling line. During all other cruises, this export ratio is < 2–10%, with an increase near shore where POC fluxes are generally elevated. Also, during the Spring Intermonsoon, a POC export maximum is observed along the northern sampling line. Both this Spring export feature and late-SW Monsoon flux maximum appear to be associated with a phytoplankton community structure dominated by diatoms. The timing of the late-SW Monsoon flux peak agrees with the observed flux maximum in the deep moored time-series sediment traps (Honjo et al., 1998). This dramatic increase in export between the mid- and late-SW Monsoon also corresponds to measured decreases in the stocks of total organic C in the upper 150 m (Hansell and Peltzer, 1998) and a sharp decline in surface water Al and Fe (Measures and Vink, 1998). These 100 m flux results, plus a series of POC flux profiles, allow for a more complete understanding of the magnitude and timing of sub-euphotic zone export in the Arabian Sea.

* Corresponding author. Tel.: 001 508 457 2000; fax: 001 508 451 2193; e-mail: kbuesseler@whoi.edu.

0967-0645/98/$ – see front matter
PII: S0967-0645(98)00078-2

1. Introduction

The Arabian Sea is known to be a region of strong seasonal reversals in surface circulation driven by the monsoonal winds (Bauer et al., 1991; Bruce et al., 1994). These physical processes are postulated to support high primary production levels due to the enhancement of nutrient supply. Observations and models in this region now generally support this hypothesis (Gallacher and Rockford, 1995; McCreary et al., 1996; Bartolacci and Luther, 1998). In addition, the seasonal patterns in surface production are thought to drive the strong seasonal variations in deep particle fluxes observed in Arabian Sea sediment trap moorings (Nair et al., 1989; Ramaswamy et al., 1991; Haake et al., 1993). Less is known, however, regarding seasonal and spatial variations in shallow particle fluxes and how these respond to physical and biological processes in this region.

The focus of this study is on the naturally occurring radionuclide, thorium-234 ($t_{1/2}$ = 24.1 days). Given ^{234}Th's high particle affinity and constant source (from ^{238}U) and decay rate, ^{234}Th's activity distribution can be used to quantify fluxes and aggregation/dissaggregation rates of particles. We employ a recently developed ^{234}Th approach in order to quantify export fluxes on regional and seasonal scales (Buesseler et al., 1992a). With this approach, ^{234}Th activity measurements are used to predict vertical ^{234}Th fluxes, and the measured ratio of POC/^{234}Th on particles is used to quantify POC export from these predicted ^{234}Th fluxes. This ^{234}Th approach for quantifying upper ocean POC export has now been used by a number of scientists over a wide range of oceanographic settings (summarized in Buesseler, 1998).

The samples discussed here were collected as part of the U.S. Joint Global Ocean Flux Study's (JGOFS) Arabian Sea Process Study. The results of the present study are used to estimate the timing and magnitude of upper ocean particulate fluxes in this basin. These fluxes can then be placed in context of the larger suite of biogeochemical measurements that were made during the same cruises. A few of these ^{234}Th results have already been incorporated in a global and regional overview of the relationship between surface primary production and shallow particulate fluxes (Buesseler, 1998). A preliminary analysis of the relationship between Arabian Sea surface production, shallow export, deeper sediment trap fluxes and burial also been has made (Lee et al., 1998).

2. Sampling and analyses

2.1. Sampling locations

Samples for ^{234}Th, POC, and PON analyses were collected on four of the major process cruises sponsored by the U.S. JGOFS program in the Arabian Sea. The clock-wise cruise tracks (Fig. 1) started with a transect off shore of Oman in the Northern Arabian Sea (N-line: N1–N11), headed south to the southern-most station at 10°N, and followed a return southern transect back into the coastal region (S-line: S15–S1). The cruises are identified here by the cruise number used aboard the *R/V*

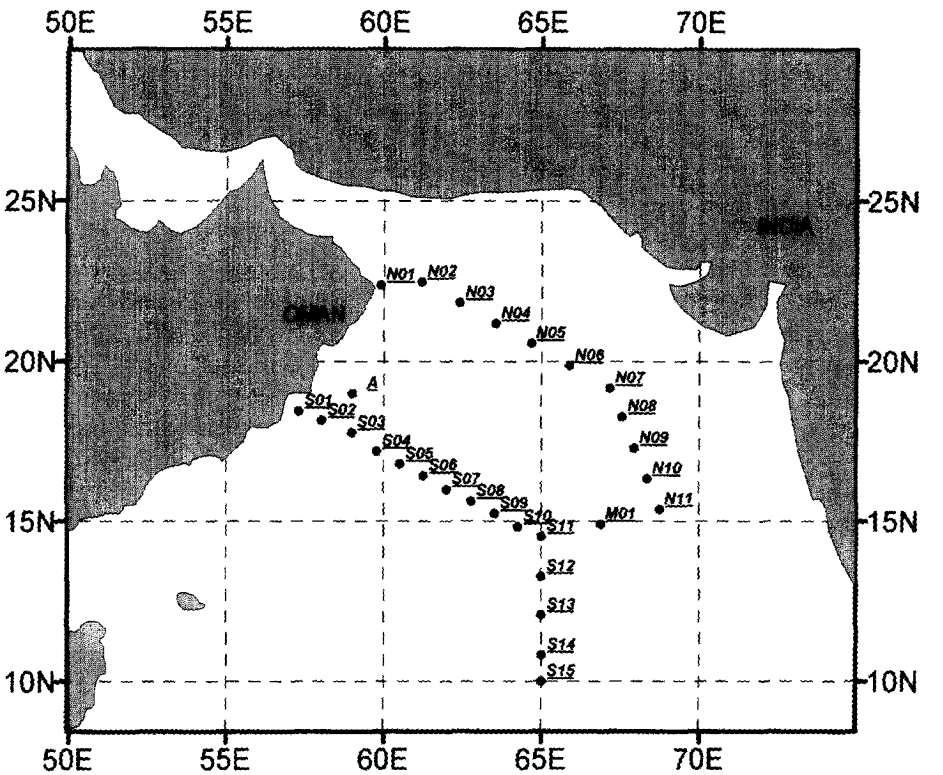

Fig. 1. Standard JGOFS Arabian Sea station location map. Note that all process cruises began at station N1 and complete the north-line to N11 and then generally continued clockwise towards S15, ending at S1 along the south-line.

Thomas Thompson and a seasonal identification based upon wind patterns at the central meteorological mooring near S07 (15.53°N, 61.50°E; Weller et al., 1998). These are: Northeast Monsoon-TN043, 8 January–4 February 1995; Spring Intermonsoon-TN045, 14 March–10 April 1995; mid-Southwest Monsoon-TN049, 17 July–15 August 1995; late-Southwest Monsoon- TN050, 17 August–15 September 1995. A few ^{234}Th data also were obtained from the early-southwest monsoon cruise (TN048, 21 June–13 July 1995). This cruise focused primarily on small-scale features and jets originating near the Oman coast along the S-line (Brink et al., 1998).

2.2. Sample collection

Samples for ^{234}Th and POC/PON were collected primarily using in situ pumping techniques supplemented by surface sampling using the ship's continuously flowing seawater line. The in situ pump was custom designed for this project to allow for maximum flexibility for large-volume sampling. The pump consisted of a positive displacement pump head that was magnetically coupled to a DC motor. A lap-top PC

was used to program the pump speed (5–15 l min^{-1}) and total volume desired for each cast. It also set the controls that terminated pumping if either battery limits were reached or filter clogging was detected based upon a slowing of the net flow rate through the filters. The pump was programmed to turn on at a preset delay time or once a pre-set pressure was reached (detected by an in situ pressure sensor). We found the pump reliable for upwards of 20–25 casts using a single battery pack, collecting $>$ 200 l during each cast.

A large part of this program relied on "vertically integrating sampling" as described in our earlier ^{234}Th studies (Buesseler et al., 1994, 1995). In this mode, the pump was lowered at a slow speed by the winch (1–3 m min^{-1}) and an in situ pressure sensor initiated pumping between a preset depth interval (here 5–100 m), sampling constant volumes over each depth interval (most often 10–20 l for every 5 m interval). With the continuous lowering of the pump and this pulsed sampling, the "Slurper" pump collected a single sample that reliably represented the average activity or concentration of a given element over the chosen depth interval. The advantage of this sampling mode was that significantly more stations and times could be sampled for the same amount of effort. Furthermore, narrowly defined vertical features were less likely to be missed relative to traditional bottle sampling. An obvious disadvantage was that discrete depth information was lost, but for the purposes of this study, this was deemed less important. At the end of each cast, a complete time-series record of flow and pressure was obtained in order to evaluate the sampling history. Sampling at fixed depths was also accomplished with the same pump by choosing a narrow depth range.

Similar to our previous JOGFS ^{234}Th sampling programs, we used 142 mm diameter filters and Mn adsorbers for the collection of particulates and dissolved ^{234}Th, respectively (Buesseler et al., 1995). In standard sampling mode, water was passed at 5–7 l min^{-1} through a 53 μm (nominal pore size) Nitex screen, followed by a 1 μm (nominal pore size) quartz filter (MQ-microquartz). The filter holder was designed such that there was no contact between the Nitex prefilter and MQ filter. A wide-mouthed, baffled opening ensured that particles were distributed evenly across both filters and were not washed off during retrieval of the pumps. When this filter holder was used in-line on the ship, the baffled opening was replaced by a top with a central connector for 3/4 in OD diameter tubing. Excess water was pulled through the filters at the end of any sampling period, and the filters were removed onto petri dishes for further processing in the lab. We define our particulate fractions operationally by the material collected by these two filters, namely, $>$ 53 μm for the Nitex samples and 1–53 μm for the MQ samples.

Dissolved ^{234}Th was defined as that fraction of the total sample that passed through the MQ filter. On the first cruise, we used separate casts for collecting sub-surface particulate and total ^{234}Th samples. On this cruise, large-volume samples were used for particulates only (300 to 500 l, Nitex screen plus MQ filter) and smaller samples were used for the collection of total ^{234}Th (50 to 100 l, MQ filter only plus 2 Mn adsorbers). During the other three cruises, single large-volume casts ($>$ 250 l) were used for the collection of Nitex, MQ and dissolved ^{234}Th (using 2 Mn adsorbers), similar to our prior studies in the Equatorial Pacific Ocean (Buesseler et al., 1995).

This change allowed us to reduce wire time and to spend more effort on each cruise determining spatial and depth related changes in the ^{234}Th activity distributions, and hence export fluxes.

Manganese adsorbers were used for the collection of dissolved Th isotopes (Livingston and Cochran, 1987; Buesseler et al., 1992b). This technique is based upon the removal of dissolved ^{234}Th using Mn coated adsorbers. The collection efficiency, E, of each adsorber pair is determined from: $E = 1 - B/A$, where A and B are the activities of ^{234}Th on the first and second adsorber, respectively. We now use 3″ tall polypropylene filter cartridges impregnated with Mn oxides as our in situ adsorbers. Details of the preparation of these adsorbers can be found in Hartman and Buesseler (1994). Collection efficiencies averaged 87 ± 7% for all of the Arabian Sea cruises.

2.3. ^{234}Th analyses

Samples for ^{234}Th were processed using both gamma- and beta-counting techniques depending upon the overall sample size and matrix. Mn adsorbers were processed using one of the two methods. On the first two cruises, Mn adsorbers were processed on board ship using a newly designed procedure. With this method, warm acid and reducing agents were recirculated through each Mn adsorber in the presence of a ^{230}Th yield monitor. This sample extract was reprecipitated by raising the pH, and the resulting precipitate was collected on a 25 mm diameter MQ filter. The precipitate was dried at 40°C overnight, mounted on a plastic counting ring, and covered by mylar and foil to allow direct detection of the energetic ^{234}Pa daughter betas (E_{max} = 2.3 MeV) which are in equilibrium with ^{234}Th. After repeated counting on the beta detectors (RISO National Lab, model GM25-5), samples were returned to the lab for re-dissolution and evaluation of the at-sea extraction yield based upon the ^{230}Th yield-monitor which was measured by inductively coupled mass spectrometry. Selected samples also were run in the lab via established radiochemical procedures using acid-based purification techniques and beta counting in standardized geometries for calibration of this sea-going technique.

The second technique used for dissolved ^{234}Th analysis is identical to that used previously (Buesseler et al., 1995). In this procedure, Mn adsorbers are dried overnight, crushed in a die for 60 s under 10 tons of pressure using a bench-top press, and the resulting 3 cm tall "puck" is counted directly for the low-energy ^{234}Th gamma using a sea-going, high-purity germanium gamma detector (Canberra 2000 mm^2 LEGe style detector). The overall detection efficiency is checked by the analyses of selected samples that are returned to the lab for complete radiochemical analyses.

The advantage of the at-sea extraction technique and beta counting method is that the procedure is highly sensitive and smaller volumes are needed. The disadvantage is that processing times at-sea are long for the extraction of Mn from the adsorbers (24 h per four samples). Since we were limited to a single cruise participant, the less labor-intensive method was chosen. Fundamentally, beta techniques are more sensitive since each ^{234}Th beta decay can be detected with > 30% overall efficiency, while only 4% of the beta events lead to a gamma signal (at 63 KeV), and these events are detected with a low efficiency (< 2%).

Given the lower activities of ^{234}Th on the MQ (10–30% of total) and Nitex filters (1–5% of total), we employed the more sensitive beta counting techniques for the detection of ^{234}Th in all particulate samples. As in our prior studies (Buesseler et al., 1995), the fresh Nitex screen was carefully removed from the filter holder and rinsed with 50 ml of MQ prefiltered deepwater and sonicated for 30 s in order to remove particulate matter off of the screen. The sample and beaker washes were then filtered onto a pre-combusted 25 mm diameter MQ filter under vacuum and dried overnight. These filters were mounted onto a plastic counting ring, covered with mylar and foil, and counted in the same way as the Mn precipitates described above. Samples were returned to the lab for detector calibration and POC/PON analyses on the remaining filter material. Our studies in the equatorial Pacific Ocean and the Arabian Sea suggested that we were removing $>$ 80–90% of the material off of the Nitex screen. We also found that an additional 0–20% of the POC was lost to the filtrate during rinsing and sonication steps. We contend that the POC/^{234}Th ratio of the material caught on the final MQ filter is representative of the original Nitex sample, and furthermore, that any errors in the quantities of POC or ^{234}Th collected on the screens do not affect the total mass balances for these elements given the small percentage of total ^{234}Th or POC in this size class ($<$ 1–5% of the total concentration on Nitex; see Results).

The 142 mm diameter MQ filters were dried overnight at 40°C and a stainless-steel cutter and jig were used to cut out 20 subsamples, each 25 mm diameter, from the filter. These subsamples were stacked into a counting ring and pressed under low pressure (1 ton) to a constant height/geometry and covered with mylar and foil similar to the other samples. These filter stacks were directly beta-counted. Selected samples also were returned to the lab for reanalysis using standardized procedures and calibration of the at-sea counting efficiencies. The remainder of the filter was used for POC/PON analyses.

Samples that we beta-counted at-sea were always counted through a mylar and foil cover to reduce emissions from other potential low-energy beta-emitters. Samples were counted 4–6 times for a period of 2–24 h over the 1–2 months following sample collection. This allowed us to follow the natural decay of the ^{234}Th signal over background. A curve fitting procedure was then used to determine the initial decay-corrected count rate and the associated background count rate. In this manner, precision was improved and the assumption of constant background was not necessary. We found the background to be extremely constant in these samples and relatively small compared to the overall net ^{234}Th signals. All of the data reported here are decay-corrected to the mid-point of sample collection and are reported in units of disintegrations per minute per liter of seawater (dpm l^{-1}). The errors reported are a combination of counting uncertainty and detector calibration, and for dissolved ^{234}Th, include the error associated with using Mn adsorbers for determining dissolved ^{234}Th-collection efficiencies.

2.4. POC/PON analyses

As in past studies, POC and PON were operationally determined parameters representing that fraction of the total organic C and N pool that was retained on MQ

or Nitex filters. We will use the terms POC or PON to refer to the fraction retained on the MQ 1 μm filter as it is closest in practice to the commonly used GFF filters which have a nominal 0.7 μm cut-off. "Large" particulate organic carbon (LPOC) or large particulate organic nitrogen (LPON) refers to the material we collected on 53 μm Nitex screen. The transfer of material off of the Nitex screen and onto the quartz filter allowed us to measure both ^{234}Th and organic C on the same sample. As shown in past studies and stated above, this rinsing procedure may underestimate the total LPOC concentrations by 0–30%. However, given that we are primarily interested in Nitex POC/^{234}Th ratios, we do not feel that this significantly compromises our results.

Microscopic examination of the material rinsed off of the Nitex was conducted at a few stations during the mid-SW Monsoon cruise in collaboration with W. Balch. The major components appeared to be intact or broken pieces of phytoplankton, unidentified marine snow, and a rare fecal pellet. Perhaps it is more useful to point out that intact or large zooplankton were not observed, and we assume that these avoided the mouth of our in situ pump. Equivalent samples from the ship's surface seawater line (intake approximately 5 m depth) contained significant, but widely varying numbers of intact zooplankton, leading to large and often widely varying LPOC concentrations not found in the in situ pump samples.

For the analysis of POC, PON, LPOC and LPON, CHN analyses were conducted on subfractions of the dried filters using standard protocols. All samples were treated via acid fuming to remove carbonate phases, though $CaCO_3$ is thought to represent only a minor component of these POC and LPOC samples. An analysis of C/N ratios and comparisons between our pump POC and LPOC data and standard bottle filtration POC data will be made in the Results section below.

3. Results

3.1. Thorium-234 activities

Total ^{234}Th results are shown for four cruises in Fig. 2. These data are now available at the U.S. JGOFS Data System Management Office's web site (http://www1.whoi.edu/jg/dir/jgofs/). Plotted are the total ^{234}Th activities in the surface ocean (from the ship's line) and the 0–100 m activities collected using the vertically integrating pump. The range in errors reflect a combination of counting statistics and differences in sample volume and processing losses, and most errors are $< 10\%$. Since the bulk of the ^{234}Th activity is in the dissolved phase (generally > 60–90%), the error on total ^{234}Th activities is most often dominated by the error in the dissolved ^{234}Th activity determination. Surface ^{234}Th activities are lower than, or within errors equal to, the 0–100 m integrated ^{234}Th activities. Generally, ^{234}Th activities increase with depth, approaching secular equilibrium with ^{238}U by 50–150 m in the open ocean (the ^{238}U activity is shown as a horizontal line in Fig. 2). We also collected a subset of samples from a fixed depth of 100 m (data not shown). The average 100 m total ^{234}Th activity from all cruises is within 1–2% of equilibrium

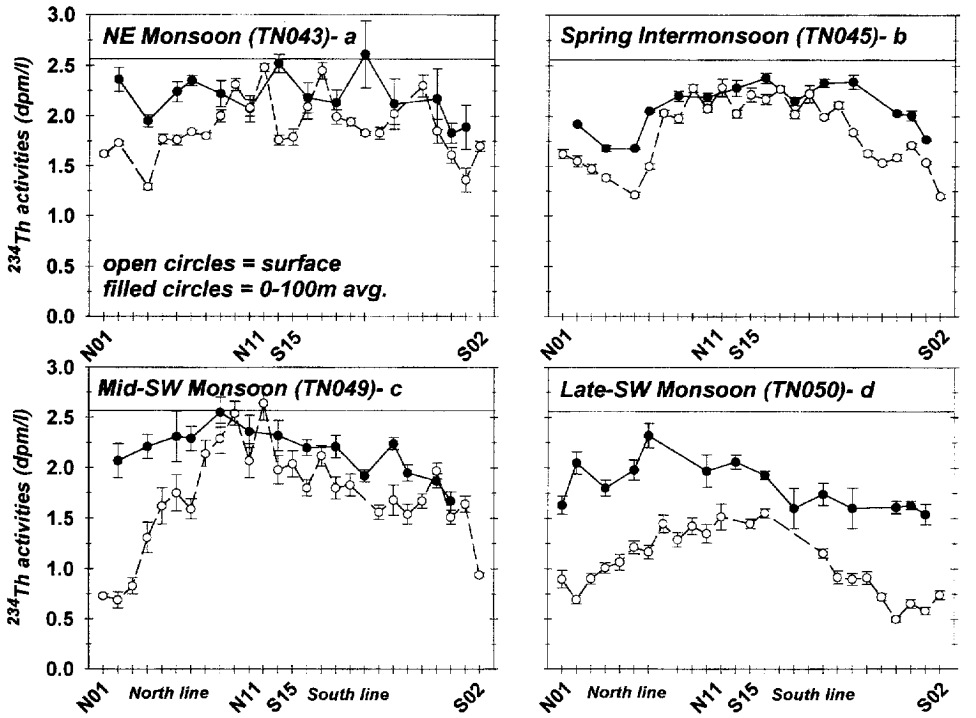

Fig. 2. Arabian Sea total ^{234}Th activities are shown for the NE Monsoon (a), Spring Intermonsoon (b), mid-SW Monsoon (c) and late-SW Monsoon (d). Shown are the total ^{234}Th activities from the surface collected from the ship's line (open circles) and the 0–100 m average activities as measured using our vertically integrating in situ pump (filled circles). Units are dpm l^{-1}, decay corrected to the mid-point of sampling and error bars are shown if larger than the symbol size.

with ^{238}U, though some samples are found with a significant depletion or excess of ^{234}Th at depth, indicating either a continued net increase or decrease in particle flux, respectively, at the 100 m horizon.

We observe both substantial regional and temporal trends in the ^{234}Th activity patterns (Fig. 2). Since low ^{234}Th indicates high particulate fluxes, the first-order interpretations of these data are: (1) particulate export rates are highest in surface waters (removal rate per liter) and decrease at depth; (2) fluxes are highest near shore at stations N1–N7 on the N-line, and S2–S11 on the S-line; and (3) the lowest activities and hence highest fluxes are associated with cruise TN050 during the latter part of the SW Monsoon. We will use these trends in total ^{234}Th from 0–100 m to quantify the particulate ^{234}Th export flux below, and then use these fluxes to derive POC export.

When profiles of ^{234}Th are used to calculate the integral ^{234}Th activity between 0–100 m, they agree very well with the activities collected using our vertically integrating sampling procedures (profile/pump $= 1.00 \pm 0.11$; $n = 6$). These results indicate that our vertical sampling technique collected total ^{234}Th samples that are representative of the local mean. Also, it implies that these results are not dominated by localized

patchiness in ^{234}Th, since these profiles and "Slurper" samples are collected on different casts that are separated by at least one hour, and more often up to 6–12 h. In addition, replicate "Slurper" casts conducted at the same station agree within errors for both total ^{234}Th and the particulate fraction. Total ^{234}Th activities collected from the ship's line also agree with the total collected by our in situ pump when deployed at 5m (ship's line/pump = 1.09 ± 0.19; n = 5 on TN049), though there were significant variations in the percent ^{234}Th caught on the Nitex filters using the ship's line relative to the in situ pump.

As stated earlier, particulate activities are generally a minor component of the total ^{234}Th activity at any given site. Nitex ^{234}Th activities are the smallest fraction of the total, representing < 1–5% of the total ^{234}Th activity. Exceptions to this were found in the ship's line when on occasion up to 30% of total ^{234}Th activity was found on the Nitex screens. During TN049, we conducted a specific comparison of the ship's line and in situ pump at 5 m for dissolved and particulate ^{234}Th. This experiment indicated that the total ^{234}Th activities agreed quite well between sampling systems, but that the fraction collected on the Nitex prefilter was systematically higher from the ship's line relative to the in situ pump (ship's line is 3 to 10 times higher relative to the in situ pump for ^{234}Th on Nitex). As mentioned previously, microscopic examination of these Nitex screens during TN049 indicated that more intact zooplankton were present in the ship's line. Our LPOC data showed this same trend, with higher Nitex LPOC concentrations on samples collected via the ship's line relative to the in situ pump (ship's line 4 to 10 times higher for LPOC on Nitex relative to in situ pump). In any case, the total ^{234}Th data from the ship's line were comparable to our pumps, and hence these total activities can be used to extend in space and time our ^{234}Th measurements from the in situ pumps. We consider our in situ pump samples to be equivalent to bottle samples, where active avoidance by large zooplankton reduces overall zooplankton abundances. Given these concerns, we do not rely on the ship's line for accurate prediction of particulate ^{234}Th and LPOC concentrations, and furthermore, these surface POC/^{234}Th ratios are not used to calculate any of our export fluxes.

The MQ fraction generally accounts for 10–40% of the total ^{234}Th activity, with the highest particulate fractions found in surface waters. On our first cruise (TN043), however, we noticed a systematic trend in the fraction of ^{234}Th collected on MQ filters related to the sample volume. During this cruise, samples for total ^{234}Th were collected from 50–100 l volumes (MQ only plus Mn adsorbers) while separate casts were used for larger volume samples (> 200–500 l) which were analyzed for Nitex and MQ particulates only. In the surface waters, sample volumes for total ^{234}Th averaged 100 l, while separate Nitex and MQ samples averaged 290 l. The 100-liter MQ sample ^{234}Th activity was systematically 50% higher than their 290 l counterpart (n = 10; comparing MQ only with sum of MQ & Nitex ^{234}Th for the large volume samples; i.e. both are nominally > 1 μm particulate fractions). For subsurface water, the differences in volume were larger, and the ^{234}Th MQ activities collected on 49 l samples were on average 2.7 times higher than for the larger 490 l samples (n = 11). Interestingly, we did not see this same volume related effect on the Nitex screens for either ^{234}Th or LPOC (n = 3), or for the MQ filters for POC.

These results and unpublished data from this lab suggest that MQ filters retain a small fraction of the "dissolved" ^{234}Th sample activity. The volume-related bias suggests to us that this is a sorption-based/site-limited phenomenon in which nominally dissolved ^{234}Th is retained on the MQ at specific sorption sites. We postulate that these sites are saturated quickly, after which the filter begins to act as a more representative particle collector (i.e., the bias becomes less significant at higher volumes). This is the opposite effect one would expect if the filter is becoming clogged and thus the effective pore size is decreasing with increased loading.

This effective retention of at least some fraction of dissolved ^{234}Th on the MQ filter is perhaps similar to observations found for POC analyses. For example, it has been shown that when two GFF filters are placed in series, the second filter will retain additional OC that has originally passed through the first filter. Whether this is primarily related to physical or chemical retention of filter-passing OC is difficult to determine. This is one argument in the ongoing discussions of why large volume, in situ, POC pump data are generally lower than equivalent small volume POC data derived from bottle sampling. In one case in the Arabian Sea where double MQ filters were mistakenly stacked in our filter holders, we measured POC on the second filter equivalent to 20% of that retained on the first one. For this same sample, a ^{234}Th activity equivalent to 48% of the first filter was caught on the second MQ filter, indicating that regardless of the mechanism, ^{234}Th data on MQ are more prone to this sorption effect than POC. Although "excess" MQ ^{234}Th would decrease the fraction collected downstream as "dissolved" ^{234}Th, the total ^{234}Th activity would remain unaffected.

In the discussions below, we rely on total ^{234}Th activities to predict net export and the 100 m POC/^{234}Th ratio on Nitex screens to predict POC fluxes. It is thus important to reiterate that we see no evidence that the total ^{234}Th activities are affected adversely by this MQ sorption phenomenon. Furthermore, it is only an issue for the rather small set of 50 l ^{234}Th samples collected on TN043. Regardless, this bias would not effect the POC and ^{234}Th concentrations collected on the Nitex screens at 100 m that are used in the calculation of POC export.

3.2. Particulate organic carbon and nitrogen

As with the particulate ^{234}Th results, POC and PON samples were collected primarily from surface waters via the ship's line or using the in situ pump to obtain either 0–100 m integrated samples or a sample from a fixed depth, most commonly 100 m. For our study, the primary data of interest are the LPOC results from 100 m, as these are used to fix the POC/^{234}Th ratio of particles exiting the upper 100 m layer. For calculating POC fluxes, we focus on these 100 m Nitex samples, as we assume that the material caught on this large pore size screen is most representative of the sinking pool.

As with particulate ^{234}Th, POC concentrations are generally higher in the surface waters and in the near shore stations, decreasing with depth for either the MQ or Nitex screen fractions. Large particulate organic carbon, i.e. particulate OC on the Nitex screens, is generally 2–10 times lower than the MQ POC, with the exception of

a few of the ship's line samples. At 100 m, LPOC concentrations show some station to station variability but no clear seasonal trend, ranging from < 0.05 μmol l^{-1} to > 0.25 μmol l^{-1}. POC concentrations at 100 m range from roughly 0.5 to > 2.5 μmol l^{-1}.

We can compare our 100 m POC concentrations to POC collected via standard bottle casts followed by filtration in the lab. In addition to sampling differences (pump vs. bottle), it should be noted that the bottle-based POC's were collected on precombusted GFF filters and from smaller, 2–4 l samples collected on separate CTD casts. The most appropriate comparison can be made at fixed depths where both techniques were used. We therefore compare the 100 m bottle POC's (> 0.7 μm) to the sum of our MQ and Nitex POC's (i.e. > 1–53 μm plus > 53 μm fractions) from our in situ pump. These data are only available from TN043, TN045 and TN049, as during the late-SW Monsoon cruise, TN050, no bottle POC's were collected. Particulate organic carbon at 100 m generally ranges from 0.2 to 2.5 μmol l^{-1}, with an overall mean of 1.9 μmol l^{-1} for the bottles and 1.5 μmol l^{-1} for the in situ pump. The trend of slightly higher values of POC from the bottle may reflect the smaller cut-off for the GFF vs. MQ filters and the presence of smaller picoplankton at many these stations. Preliminary biomass results would tend to support this inference (L. Cambell, personal communication).

The focus of this paper is on the quantification of POC export from the upper 100 m. Using C/N ratios, it is also possible to predict PON fluxes directly from these results. C/N values for the Nitex screens tend to be slightly higher than on the MQ filters (for example, molar ratio C/N = 6.6 vs. 6.1 for all surface Nitex and MQ filters, respectively). The Nitex screens used here in the export calculations also show a general increase in C/N ratios with depth (C/N average for all cruises = 6.6 at surface and 7.5 at 100 m). This is consistent with the preferential remineralization of particulate N over C with depth, as seen in other studies.

4. Discussion

4.1. Thorium-234 export fluxes

The activity balance of total ^{234}Th in the ocean can be described by the following equation:

$$\delta A_{Th}/\delta t = A_U\lambda - A_{Th}\lambda - P + V \quad (1)$$

where A_{Th} and A_U are the activities of ^{234}Th and ^{238}U, respectively; $\delta A_{Th}/\delta t$ is the time rate of change of ^{234}Th; P is the net vertical loss of ^{234}Th on sinking particles; and V is the sum of advective and diffusive terms. ^{238}U is conservative in seawater, and hence from measurement of salinity, this activity can be calculated (Chen et al., 1986).

In prior studies, $\delta A_{Th}/\delta t$ is most often set to zero, as single measurements necessitate the assumption of steady-state, i.e. the calculated ^{234}Th flux is assumed to be constant over the mean life of ^{234}Th, 35 days. This assumption has been shown to provide adequate resolution of ^{234}Th fluxes in most settings except during major short-lived

bloom events (Buesseler et al., 1992a; Cochran et al., 1997). Given the large variations in particle flux expected in the Arabian Sea, we take an approach similar to Buesseler et al. (1992a), and use the time-series data at any given station to estimate of $\delta A_{Th}/\delta t$ at each point in space and time calculated from the total activity difference between sampling periods. For the first cruise, TN043, we must assume steady-state conditions, since we have no prior activity data. As will be shown below, the magnitude of this correction is small at all sites and cruises except between the mid- to late-SW Monsoon period when we see a major flux increase (between TN049 and TN050).

The V term in Eq. (1) includes vertical and horizontal advective and diffusive processes. In the vertical dimension, the upwelling of waters high in ^{234}Th activity provides a net source of ^{234}Th that must be balanced in Eq. (1) by additional particulate export. Similar to our studies in the equatorial Pacific (Buesseler et al., 1995), we have added an upwelling term to our flux model ($V = w \cdot \delta A_{Th}/\delta z$ in Eq. (1)). The vertical activity gradient of ^{234}Th is approximated from the 100 m and 0–100 m activities, and a modeled upwelling velocity, w, at 100 m is used. Upwelling is derived from a circulation model based on the Modular Ocean Model (MOM, Pacanowski et al., 1991) with the vertical mixing scheme of Pacanowski and Philander (1981). The model domain covers the global ocean from 80°S to 80°N with realistic geometry and bottom topography. The horizontal resolution is 2°s longitude and 1° latitude, and there are 22 vertical levels. After a ten years spin up forced by the climatological air–sea fluxes (Hellerman and Rosenstein, 1983; Levitus, 1982), the model was integrated from 1992 to 1996, forced with daily air–sea fluxes derived from National Center for Environmental Prediction (NCEP) analysis (see Chao and Fu, 1995 for detailed descriptions). The model output was saved as three-day snapshots, and the 1995 results for w were averaged over the mean life of ^{234}Th and used in the present study.

Scaling arguments can be used to demonstrate that advection would dominate over diffusion in the transport of ^{234}Th along horizontal gradients in the open ocean (Buesseler et al., 1994). We used the measured ^{234}Th activities to derive horizontal activity gradients, and multiplied these by estimated horizontal advective velocities as a first-order estimate of the relative strength of horizontal transport. As with the upwelling velocities, the advective velocity for the upper 100 m was derived from our model simulations. The modeled horizontal velocities generally agree with measured ADCP data (Flagg and Kim, 1998). When averaged over 0–100 m and the mean life of ^{234}Th, these horizontal velocities are small, $< 10\,cm\,s^{-1}$, but surface maximum velocities can reach $80\,cm\,s^{-1}$ or more. On average, the calculated horizontal flux term was $< 15\%$ of the net export flux of ^{234}Th. As such, we neglect this small term in the following flux calculations. A similar conclusion was reached in prior ^{234}Th activity balances in the equatorial Pacific (Buesseler et al., 1995), though horizontal transport of ^{234}Th may be significant in near-shore environments and coastal harbors (Gustafsson et al., 1998). Our inability to tightly constrain horizontal fluxes of any constituent in space and time remains a challenge in all mass balance calculations in ocean sciences.

Thorium-234 fluxes for each of the cruises are shown in Fig. 3a–d. We show these fluxes as a series of bars separating out the flux at 100 m calculated on a $dpm\,m^{-2}\,d^{-1}$ basis into the "steady-state" term (i.e. $(A_U - A_{Th})\lambda$), the "upwelling" term (i.e.

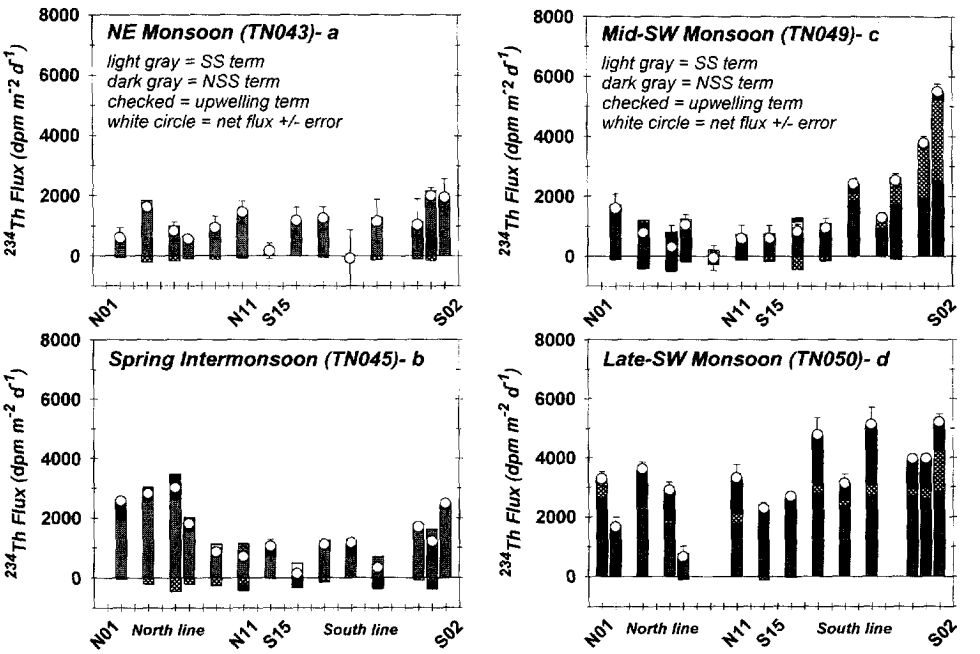

Fig. 3. Arabian Sea ^{234}Th fluxes are shown for the NE Monsoon (a), Spring Intermonsoon (b), mid-SW Monsoon (c) and late-SW Monsoon (d). Each stacked bar depicts the magnitude of the three main terms in Eq. (1), namely the steady state term (SS- light gray), non-steady state term (NSS- dark gray) and upwelling term (checked). The ^{234}Th fluxes at 100 m are calculated in units of dpm $m^{-2} d^{-1}$ such that a sinking flux out of the upper 100 m is shown as a positive flux, and a source of ^{234}Th due to upwelling is shown as a negative flux (i.e. opposite of vertical export). The net ^{234}Th flux calculated from the full model is shown with the associated error (white circle). Note that in most cases, the SS term is the largest contributor to the net flux. During the mid-SW Monsoon, upwelling becomes highly significant at stations S2–S3 (checked bars, 3c) and during the late-SW Monsoon, the NSS terms becomes important (dark gray bars, 3d).

$w \cdot \delta A_{Th}/\delta z$), the "non-steady-state" term (i.e. $\delta A_{Th}/\delta t$) and the "net" ^{234}Th flux, which is the mathematical sum of the three. In this manner, it is easy to see what terms in Eq. (1) drive the net ^{234}Th flux used in calculating POC export. The error bar shown on the net ^{234}Th flux is a based upon an estimate of the flux errors, due to the analytical uncertainty on our ^{234}Th measurement.

Focusing on the net ^{234}Th flux first, net fluxes are seen to range from zero (i.e. within errors, sinking losses of ^{234}Th are too low to quantify on the time scale of this tracer) to > 5000 dpm $m^{-2} d^{-1}$. For comparison, ^{234}Th fluxes in the 1000–2000 dpm $m^{-2} d^{-1}$ range are similar to those measured in the equatorial Pacific Ocean, and values > 3000 are comparable to those found during the North Atlantic Bloom Experiment (Buesseler et al., 1992a, 1995). Fluxes of < 1000 dpm $m^{-2} d^{-1}$ are similar to mean fluxes at Bermuda, and indicate relatively small net export at 100 m (Buesseler et al., 1994, Buesseler, 1998).

Overall, there are clear spatial and seasonal trends in the net ^{234}Th flux pattern. Net ^{234}Th fluxes tend to be higher near shore along both the north and south lines. During the NE Monsoon (TN043), fluxes are generally low throughout the basin, with perhaps a flux minimum at the southernmost station S15 (note, the minimum at S9 is associated with a very large uncertainty). During the Spring Intermonsoon (TN045), an elevation in net ^{234}Th export is seen along the N-line near shore (N2–N7), with the lowest values found offshore along both the N- and S-line. The S-line shows an increase in net export closely associated with the inner-most stations only (S2–S4). During the mid-SW Monsoon (TN049), we actually see a slight decrease in export along the N-line stations N2–N7, and then a more wide-spread elevation in export along the S-line from S3–S9 relative to the Spring cruise. The most dramatic seasonal shift in export occurs during the late-SW Monsoon (TN050) when across the entire basin, export fluxes are elevated relative to the other cruises, approaching some of the highest net export values for ^{234}Th reported to date.

Throughout the year and at most sites, the net ^{234}Th flux can be predicted from the simple steady-state model, since the magnitude of the other terms are insignificant (Fig. 3). Exceptions to this pattern are found during the mid-SW Monsoon (TN049) when near-shore upwelling along the S-line requires us to almost double the predicted net export of ^{234}Th to balance the ^{234}Th supply from below (stations S3 and S4; Fig. 3c). The enhancement of upwelling nearshore during this time period is not unexpected, and is a major feature of the physical forcing in this basin which enhances nutrient supply along the margins.

The only other significant variations in predicted ^{234}Th fluxes from the steady-state model occur during the late-SW Monsoon, when the non-steady-state (NSS) term can lead to a doubling of the calculated vertical ^{234}Th flux (Fig. 3d). In essence, given the activity patterns shown in Fig. 2, the observed basin-wide decrease in ^{234}Th between the mid- and late-SW Monsoon requires that net vertical export be enhanced in order to balance not only ^{234}Th production and decay, but also to support a drop in overall ^{234}Th activities in the upper 100 m. We conclude that the general magnitude of net ^{234}Th export in the late-SW Monsoon, determined by the full NSS model, is our most accurate estimate of ^{234}Th flux; however, station-to-station variability in these fluxes may be related to the assumption that we are following single parcels of water over time.

Quantitatively, the NSS ^{234}Th fluxes shown in Fig. 3a–d are used to calculate POC export below. Qualitatively, these seasonal export patterns are consistent with many other biogeochemical rate and stock measurements made during the Arabian Sea Process Study, many of which are presented in this volume. For example, preliminary examination of ^{234}Th fluxes indicates that enhanced ^{234}Th export is correlated with the increased abundance of large diatom blooms as measured by pigment distributions in the Arabian Sea (Latasa and Bidigare, 1998). For example, the overall increase in ^{234}Th export along the N-line during the Spring Intermonsoon and the large basin-wide export peak during the late-SW Monsoon fit this pattern quite well (R. Bidigare, R. Goericke personal communication). Similarly the timing of the major export peak, with a basin-wide flux maximum only late in the SW Monsoon, fits the timing of the deep ($>$ 500 m) sediment trap export maximum (Honjo et al., 1998). This

shallow export maximum also coincides with dramatic decreases in surface Al (Measures and Vink, 1998) and total organic C (Hansell and Peltzer, 1998). Further analyses and comparison of these data sets are currently underway.

The only other published Arabian Sea ^{234}Th results for direct comparison are confined primarily to the Indian coast, but they do extend fairly close to our stations N5–N7, and S15–S10 (Sarin et al., 1994, 1996). Sarin et al. have limited ^{234}Th data from 1988, 1994 and 1995, and in 1995 their fluxes at 100 m for ^{234}Th ranged from 1250 to 2050 dpm m^{-2} d^{-1}, with an increase between the Spring Intermonsoon and the mid- to late-SW Monsoon ($n = 2$ for comparable stations for both seasons), similar to those found here. However, it is difficult to directly compare ^{234}Th data collected by these other investigators, given the strong seasonality and spatial variability found in our data between back-to-back cruises during the summer months.

4.2. *Export of POC derived from ^{234}Th: background*

Earlier studies of ^{234}Th noted the similarities between ^{234}Th distributions and fluxes and general biological processes (Bruland and Coale, 1986; Coale and Bruland, 1987). Eppley (1989) suggested that one method to determine new production would be to use particulate ^{234}Th residence times to calculate POC export. As noted by Murray et al. (1989), however, POC and particulate ^{234}Th residence times are not necessarily the same (i.e. POC may be more efficiently recycled, leading to longer residence times in the surface ocean). To overcome this limitation and to still employ ^{234}Th as a quantitative POC export tracer, Buesseler et al. (1992a) showed that since the ^{234}Th flux can be derived from ^{234}Th activity distributions, POC export can be derived simply by multiplying the net ^{234}Th flux by the empirically determined POC/^{234}Th ratio on sinking particles. The applicability of this approach has now been shown in a wide variety of oceanic settings (Buesseler et al., 1992a, 1995; Shimmield et al., 1995; Bacon et al., 1996; Murray et al., 1996; Cochran et al., 1995; 1997; Rutgers van der Loeff et al., 1996; Charette and Moran, 1998), many of which are summarized in Buesseler (1998). The technique also has been expanded to include studies of the sinking particulate fluxes of other elements, such as polycyclic aromatic hydrocarbon and polychlorinated biphenyl fluxes in the coastal environment (Gustafsson et al., 1997, 1998).

The overall accuracy of this approach depends upon the reliability of the ^{234}Th flux prediction and the POC/^{234}Th ratio used in the POC flux calculation. In general, the quality of the ^{234}Th flux estimate relies primarily on the accuracy and precision of the ^{234}Th activity measurements, and not the chosen flux model. This comment is based upon studies that have shown that under most conditions (including most of the data shown here), the magnitude of the ^{234}Th flux is not strongly influenced by temporal or physical supply/loss terms in the ^{234}Th activity balance (Tanaka et al., 1983; Wei and Murray, 1992; Buesseler et al., 1995; Gustafsson et al., 1998). Rather, it is the disequilibrium between ^{238}U and ^{234}Th that is most important (i.e. $(A_U - A_{Th})\cdot\lambda$ in Eq. (1)). The POC/^{234}Th ratio does show regional, seasonal, and depth-related variability that is mechanically much less well understood. For each application of this approach, a site-specific measurement of POC/^{234}Th is required. Recent

modeling efforts of observed POC/^{234}Th ratios as a function of particle size suggest that the POC/^{234}Th ratio of large particles is determined primarily by particle coagulation kinetics (Burd et al., 1998), but our Arabian Sea data do not fit this model. We feel it is difficult to separate physical from biological effects on the resulting POC/^{234}Th ratio observed in the field studies to date.

Particulate material to be analyzed for POC/^{234}Th ratios has been collected primarily using in situ pumping techniques, and to a lesser extent, shallow sediment traps. All of these operational procedures are in agreement on the large-scale features, i.e. POC/^{234}Th ratios are highest in blooms or where community structure is dominated by short food chains/large cells such as diatoms, and this ratio decreases with depth as POC (or PON) is preferentially remineralized from sinking particles (summarized in Buesseler, 1998). When using filtration techniques it is best to measure both POC and ^{234}Th on the same filter, thus removing biases due to variations in the collection efficiency of different particle types as a function of filter type or loading. While the accuracy of shallow sediment traps for quantifying sinking particle fluxes has been called into question (Buesseler, 1991), some researchers believe that shallow traps may still be used to collect representative sinking material for POC/^{234}Th analysis (Murray et al., 1996). The only assumption we make is that our sampling techniques do not miss a fraction of sinking particles that is both dominant in the total sinking flux and vastly different in its POC/^{234}Th ratio.

There are generally smaller differences at a given depth and time in the POC/^{234}Th ratio collected by any technique relative to seasonal and depth related variability (Buesseler, 1998). Thus, the trends with space and time in any individual study would hold even if the absolute value of POC export at any site is offset due to a possible sampling bias. We focus below on the POC/^{234}Th ratios of the Nitex screens at 100 m, since we feel these are most likely to be representative of the rapidly sinking detrital pool; however, we also will comment on how this ratio varies between the Nitex and MQ filters.

4.3. POC/^{234}Th ratios in the Arabian Sea

POC/^{234}Th ratios range from > 20 to < 1 μmol dpm^{-1} in all samples from all cruises, depths and filter types during the Arabian Sea Process Study. As stated above, these ratios generally decrease with depth (Fig. 4) and are generally higher on the Nitex screen relative to the MQ filters (for example, overall POC/^{234}Th ratio on Nitex is 3 × MQ on TN050, 100 m data). At the surface and in some of the 0–100 m samples, there is a tendency for an increase in POC/^{234}Th near shore, but this pattern is not evident in the deeper 100 m samples (Fig. 5a–d). By 100 m, ratios on the Nitex screen are relatively constant around 2–5 μmol dpm^{-1}, with some higher scatter overall during the late-SW Monsoon. Since we did not collect 100 m POC/^{234}Th ratio samples at every station, we used the POC/^{234}Th ratio for any given cruise averaged separately for the N- and S-line (see horizontal lines in Fig. 5). This averaging makes little difference to the final flux estimates, except perhaps during TN050, when there was a wider range in the observed 100 m POC/^{234}Th ratios. Again, our assumption is that those particles caught on the Nitex screen are composed of detrital material that

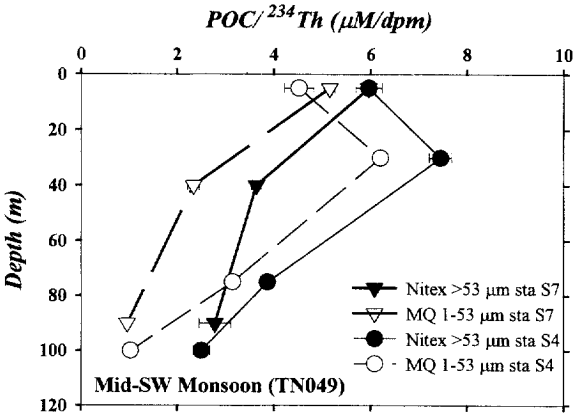

Fig. 4. Example of vertical profiles of POC/^{234}Th (units of μmol dpm^{-1}) for particulate material collected on a Nitex screen (filled symbols) or MQ filter (open symbols) from two stations along the S-line during TN049.

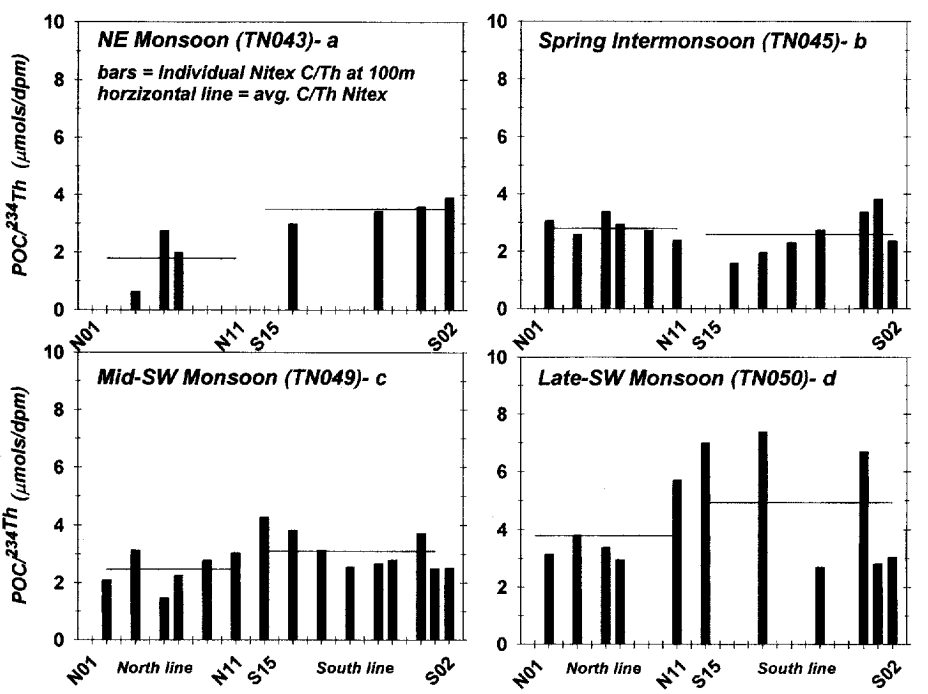

Fig. 5. Summary of POC/^{234}Th ratios collected at 100 m on Nitex screen for the NE Monsoon (a), Spring Intermonsoon (b), mid-SW Monsoon (c) and late-SW Monsoon (d). Individual ratios are shown as solid bars in units of μmol dpm^{-1}, and the average for the N- and S-line as used in the POC flux calculations is shown as a horizontal line.

is likely to be representative of the sinking flux. In addition, given the evidence of at least some dissolved ^{234}Th sorption onto the MQ filters, we are hesitant to rely on the MQ ratio as these POC/^{234}Th values would be artificially lowered by this bias. In prior studies, Nitex POC/^{234}Th values are generally lower than values measured on GFF or other filters with small pore size (Buesseler et al., 1995; Bacon et al., 1996; Burd et al., 1998), but we see the reversal of this pattern in the Arabian Sea. We feel that this may simply be a reflection of the presence of abundant large diatoms in the Arabian Sea. If these large diatoms are caught on our Nitex screens they would have a high volume relative to surface area ratio, and hence elevated POC/^{234}Th ratios would be expected, as seen in general at high latitude sites (Cochran et al., 1995; Rutgers van der Loeff et al., 1996).

4.4. POC fluxes in the Arabian Sea

POC fluxes calculated from the ^{234}Th fluxes shown in Fig. 3, and the POC/^{234}Th data in Fig. 5 are provided for each station and cruise in Table 1. The overall patterns in POC flux echo the patterns in the ^{234}Th flux distribution since the ^{234}Th flux gradients in space and time are much greater than any changes in the POC/^{234}Th ratio throughout the year at 100 m (Fig. 6a–d). In magnitude, POC flux ranges from < 1 to over 24 mmol m^{-2} d^{-1}. Particulate organic carbon fluxes tend to increase nearshore, and significant seasonal differences are seen, such as the elevated POC fluxes along the N-line during the Spring Intermonsoon (Fig. 6b). The single largest feature in this data is clearly the POC export maximum during the late-SW Monsoon at all stations, particularly along the S-line (Fig. 6d).

Increased winds in the Arabian Sea associated with the SW Monsoon started around 1 June 1995, as measured on a meteorological buoy near S7, and this wind pattern continued until October 15th (Weller et al., 1998). These winds cause enhanced coastal upwelling and hence an increase in the supply of nutrients to surface waters. This physical event is thought to trigger the onset of the summer phytoplankton bloom. Barber et al. (1998) measured enhanced primary production rates along the S-line during the mid-SW Monsoon (TN049). At this time, export fluxes are still relatively low. Therefore, there appears to be a significant delay between the onset of the SW Monsoon, increased primary production and the export of particulate matter from the surface ocean. Since we do not have continuous primary production or ^{234}Th data it is difficult to estimate the exact delay time (and this may vary spatially), but at least 30 days and up to 2 months would have passed between the start of the summer bloom period and the enhanced basin-wide export fluxes. The observed response of the deep traps in 1995 would support this one to two month delay (Honjo et al., 1998). A similar, but shorter delay was observed using ^{234}Th in the North Atlantic bloom experiment (NABE). During NABE, the onset of stratification in the spring led to a rapid increase in primary production, and roughly a two week delay in particle export was documented using ^{234}Th (Buesseler et al., 1992a). The delay in export during the seasonal bloom cycle can be thought of as being related to the relative balance between phytoplankton production and zooplankton grazing. In the NABE, the onset of increased export coincided with a depletion in dissolved Si

Table 1
Arabian Sea POC flux, primary production and export ratios

Station	NE Monsoon			Spring Intermonsoon			Mid-SW Monsoon			Late-SW Monsoon		
	TN043 POC flux (1)	TN043 P. prod. (2)	TN043 Th*E* (3) (%)	TN045 POC flux (1)	TN045 P. prod. (2)	TN045 Th*E* (3) (%)	TN049 POC flux (1)	TN049 P. prod. (2)	TN049 Th*E* (3) (%)	TN050 POC flux (1)	TN050 P. prod. (2)	TN050 Th*E* (3) (%)
N01												
N02	1.1			7.3			4.0			12.5		
N03										6.4		
N04	2.9			8.0			2.0					
N05										13.8		
N06	1.5			8.5			0.8					
N07	1.0	89.9	1.1	5.1	107.8	4.8	2.6	78.8	3.3	11.0		
N08										2.5	52.5	4.8
N09	1.7			2.4								
N10							− 0.2					
N11	2.6			2.0			1.5					
M01										12.6		
S15	0.6	53.3	1.1	2.7	63.8	4.3	1.9	130.1	1.4	11.3	51.2	22.1
S14												
S13	4.1			0.3			2.6					
S12										13.3		
S11	4.4	83.7	5.2	2.9	70.4	4.1	3.0	129.0	2.3	23.7		
S10												
S09	− 0.3			3.0	91.8	3.3	7.5					
S08										15.4		
S07	4.0	100.0	4.0	0.9	80.3	1.1	4.1	134.1	3.0	25.4	146.7	17.3
S06							7.9					
S05												
S04	3.6	84.7	4.2	4.4	100.1	4.4	11.8	114.8	10.3	19.6	72.2	27.2
S03	7.0			3.1			17.1			19.6		
S02	6.8	120.6	5.6	6.4	71.5	8.9		132.4		25.8	92.4	27.9
S01								130.6				

(1) POC flux at 100 m (mmol C $m^{-2} d^{-1}$) derived from ^{234}Th using full NSS model and Nitex C/Th ratios (see text for details).
(2) Primary production (mmol C $m^{-2} d^{-1}$) taken from in situ 24 h incubations as reported by Barber et al. (1997).
(3) Th*E* ratio = POC flux derived from ^{234}Th/primary production (from Buesseler, 1998).

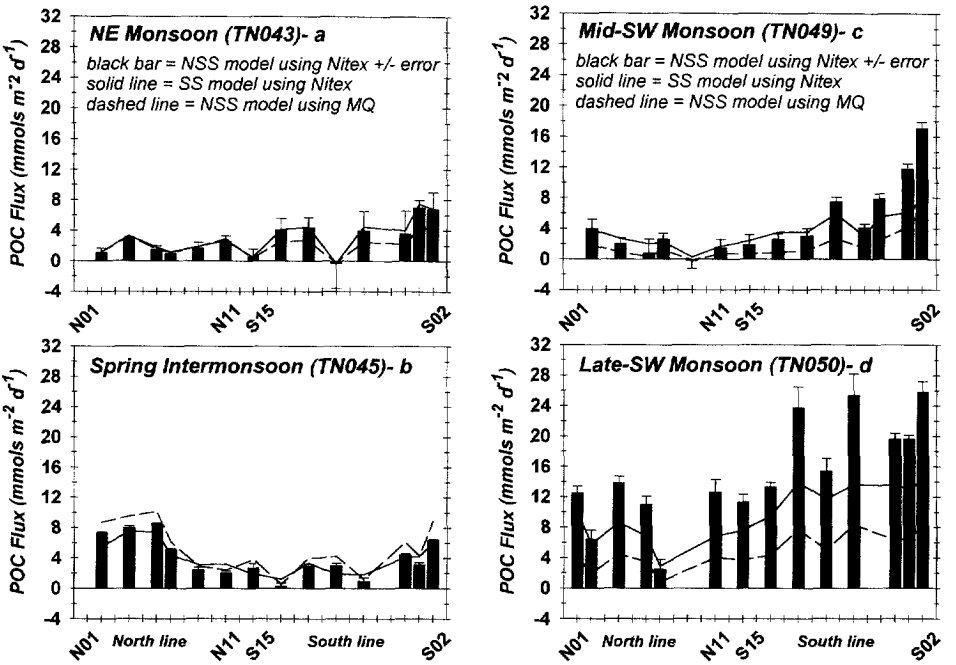

Fig. 6. POC flux at 100 m calculated for the NE Monsoon (a), Spring Intermonsoon (b), mid-SW Monsoon (c) and late-SW Monsoon (d). Fluxes are calculated in units of mmols $m^{-2} d^{-1}$ of POC export at 100 m, and the error bars are based upon the calculated ^{234}Th flux. POC fluxes are shown for the full NSS model that includes upwelling, calculated from the Nitex POC/^{234}Th ratios (solid bars). Also shown for comparison are two line plots where the magnitude of this flux is recalculated based upon the steady state model only (SS model- solid line), or employing the same full NSS model as the solid bars, but using the POC/^{234}Th ratio on the MQ filters instead (dashed line). Note that at many stations and times, all three of these estimates agree within errors, however we feel that the solid bars represent our best estimate of POC export (see text for details).

levels and the crash of a large diatom bloom. In the Arabian Sea, nitrate to silicate ratios did increase dramatically during TN050 (Morrison et al., 1998), indicating that a drawdown of Si had occurred in association with high diatom biomass.

Analogous to *f* ratios (the ratio of new production determined from nitrate uptake to total production derived from ^{14}C uptake rates; Eppley and Peterson, 1979) and *e* ratios (the ratio of trap-derived POC flux to total production; Downs, 1989), we have proposed that Th*E* ratios (the ratio of ^{234}Th derived POC flux to total production; Buesseler, 1998) can be used to examine regional and seasonal variations in the balance between C fixation in the euphotic zone and those processes that lead to particulate export. In the Arabian Sea, we find relatively low Th*E* ratios of 1–5% at N7 and at the off-shore site along the S-line (S15), with an increase to 5–10% in the near shore stations throughout the NE Monsoon, Spring Intermonsoon and the mid-SW Monsoon (Table 1). Such relatively low Th*E* ratios are common throughout most equatorial and mid-latitude oceanic settings (Buesseler, 1998). In these systems,

production and export are in close balance, indicating that primary production is tightly coupled to the efficient recycling of nutrients via the microbial loop and/or smaller zooplankton. When systems become "de-coupled", either by nutrient-limitation responses (for example, Si depletion) or zooplankton grazing effects, the biological pump can become more efficient at exporting particulate matter from the surface ocean, and this is what is seen during the late-SW Monsoon. During the late-SW Monsoon, we find particulate export ratios of 17% to $> 28\%$ along the S-line (Table 1). The only other studies where such high Th*E* ratios have been documented are during the NABE and during seasonal blooms at high latitudes (summarized in Buesseler, 1998).

Events of relatively high export, such as seen here during the late-SW Monsoon, appear to be characterized by a predominance of diatoms in the euphotic zone. In the Arabian Sea, diatoms were the predominant primary producers during the SW Monsoon and were elevated along the N-line during the Spring Intermonsoon (R. Bidigare, R. Goericke, personal communication). Enhanced POC export during the NABE was associated with the crash of a diatom bloom, which was followed by a change in the food-web structure towards smaller grazers and primary producers. High-latitude blooms are known to be dominated by high diatom abundances and associated high Si fluxes to the underlying sediments. Thus, while the exact mechanism responsible for elevated export cannot be deduced from these measurements, many regions of the world's oceans with high relative export are characterized by enhanced diatom production. Models that include simple relationships between production and export will therefore need to include at least some parameterization of these diatom-related flux events, if we are to correctly predict the export of POC and associated nutrients into mid-waters and deep-ocean sediments, where carbon can be isolated from the atmosphere on decade and longer time-scales. We will continue to examine this relationship between diatom abundances and ^{234}Th export in more detail in future publications.

In this volume, an analysis of the surface-to-sediment POC fluxes is presented for the Arabian Sea using primary production data, our ^{234}Th derived POC fluxes, the deep trap results at the five mooring sites along the S-line, and long-term sediment accumulation rates of organic carbon (Lee et al., 1998). In this paper, it is shown that the organic carbon flux decrease is quite large between the surface and 100 m, where the ratio of organic carbon fixation to POC export is typically $< 10\%$. Organic carbon flux gradients are also very steep between the deepest traps 500 m off the bottom and the underlying sediments, where POC fluxes decrease another order of magnitude (Fig. 1 in Lee et al., 1998).

During both of our SW Monsoon cruises, we collected a limited number of samples for ^{234}Th at discrete depths within the upper 100 m in order to examine the shallow depth profile of POC export in more detail. While depth resolution is often sparse, some interesting features emerge from these profiles. Shown in Fig. 7a–j are profiles of total ^{234}Th activities, POC/^{234}Th ratios on Nitex, and POC fluxes. The POC fluxes are predicted using a similar export model that includes upwelling but ignores the non-steady state term; thus, the TN050 results are likely an underestimate of the true POC fluxes (Fig. 7f–j). The ^{234}Th deficit is largest in the coastal stations, and

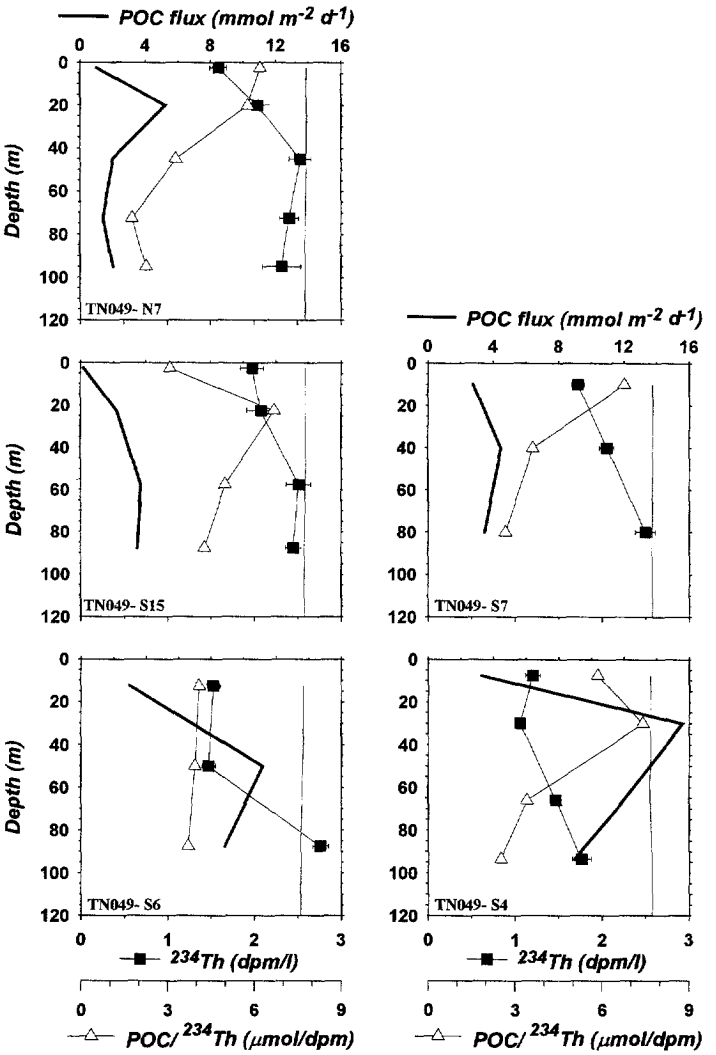

Fig. 7. Vertical profiles of total ^{234}Th activities (filled squares), Nitex POC/^{234}Th ratios (open triangles) and calculated POC fluxes (solid line) at five stations collected during the mid-SW Monsoon (a–e) and late-SW Monsoon (f–j). Station identifications are provided on each figure. Note that the POC/^{234}Th scale is more than a factor of 2 greater, and the POC flux scale a factor of 3 larger during the late-SW Monsoon (f–j). The vertical line near 2.6 dpm l^{-1} represents the ^{238}U activity.

equilibrium is not reached by 100 m at a few of these stations. The ^{234}Th flux will increase with depth until equilibrium is reached (^{234}Th flux profiles not shown). Thus, while the ^{234}Th flux may increase slightly with depth, POC/^{234}Th ratios generally decrease sharply with depth and a significant drop in the net POC flux with depth is most often predicted, indicating that shallow remineralization is occurring.

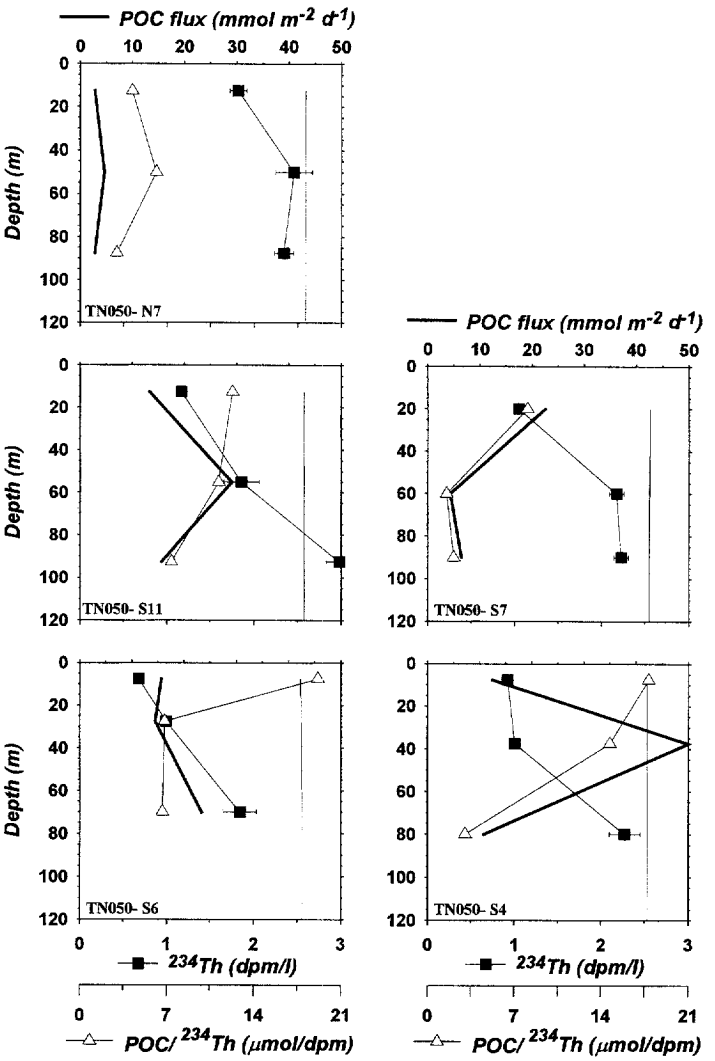

Fig. 7. Continued.

During the mid-SW Monsoon (TN049), the two coastal stations, S4 and S6, show the highest net POC export rates and a clear drop-off in POC flux from the mid-euphotic zone to 100 m. A shallow POC export maximum is also seen at N7. By the late-SW Monsoon (Fig. 7f–j; note change in horizontal scales), maximum fluxes are seen; however, POC export decreases dramatically with depth at S11 and S4, led by dramatic drop off between the mid-euphotic zone and 100 m from 50 mmol m^{-2} d^{-1} to around 10 mmol m^{-2} d^{-1} at station S4. While these profiles are not highly resolved, they do point to the importance of shallow processes on the

particle cycle, and indicate that small changes in this euphotic zone processing efficiency would lead to large changes in net export at 100 m.

5. Summary

Thorium-234 activity distributions in the Arabian Sea in 1995 are used to define the timing, spatial distribution, and magnitude of ^{234}Th and POC fluxes in the upper 100 m. New sampling procedures and stream-lined at-sea radiochemical analysis allow for considerable expansion in the use of this tracer. An important finding is that both ^{234}Th and POC export are substantially elevated during the late-SW Monsoon period. During this time period, POC export at 100 m is on the order of 15–25 mmols C m^{-2} d^{-1} along the S-line, and POC export rates are 17–27% of total primary production rates. This contrasts to other times when POC fluxes of 2–15 mmols C m^{-2} d^{-1} are predicted along the S-line, and Th*E* ratios (POC export/primary production) of < 2–10% are found. Along the N-line, the highest POC fluxes are predicted during the Spring Intermonsoon (6–8 mmols C m^{-2} d^{-1}) and the late-SW Monsoon period (2–10 mmols C m^{-2} d^{-1}). The offset in time between the onset of the summer winds and elevated export appears to be related to the onset and decline of a large diatom bloom during this summer period. The timing of this large export pulse is consistent with the continuous record in 1995 of sinking particle fluxes as measured by deep moored sediment traps along the S-line (Honjo et al., in press). Also during this time period, stocks of total organic C, Al and Fe in the upper layer decrease dramatically (Hansell and Peltzer, 1998; Measures and Vink, 1998). These decreases in concentration may be explained by enhanced export on particles. Smaller scale features are also observed, such as increased export in the near shore regions, as well as enhanced POC export along the N-line during the Spring Intermonsoon.

Thorium-234 provides a valuable geochemical tracer of particle export that can be used to derive both quantitative geochemical balances of OC and associated elements, and to increase our understanding of the processes that are responsible for enhanced particulate export in the surface ocean. The data presented here represent a first step in the more detailed analysis between the relationship between physical forcing, new production, primary production and particulate export fluxes in the Arabian Sea.

Acknowledgements

Support for this proposal came primarily from a grant to KB from the U.S. National Science Foundation. In addition, CBN was supported by an Office of Naval Research Graduate Fellowship and support for development for the "Slurper" pump was provided by WHOI's Technology Initiative Program. The circulation modeling of YC and FC was supported through the JPL Supercomputing Project. We thank the officers and crew of the *R/V Thomas Thompson* for their excellent assistance during this entire sampling program, and we acknowledge the efforts of the U.S. JGOFS Planning Office for assistance in cruise preparation and logistics. We thank S. Smith

and two anonymous reviewers for their suggestions during review. We also thank Ken Brink for providing the sampling opportunities for CBN at the start of the summer Monsoon, and Barney Balch for assistance on TN049 in microscopic examination of our samples. This is contribution #9807 from the Woods Hole Oceanographic Institution and U.S. JGOFS contribution #411.

References

Bacon, M.P., Cochran, J.K., Hirschberg, D., Hammar, T.R., Fleer, A.P., 1996. Export flux of carbon at the equator during the EqPac time-series cruises estimated from ^{234}Th measurements. Deep-Sea Research II 43, 1133–1154.

Barber, R.T., Johnson, Z., Marra, J., Bidigare, R.C., Latasa, M., Codispoti, L.A., Halperen, D., Goericke, R., Smith, S., 1998. Primary productivity and Its Regulation in the Arabian Sea during 1995. 79(1), OS29.

Bartolacci, D.M., Luther, M.E., 1998. Patterns of co-variability between physical and biological parameters in the Arabian Sea. Deep-Sea Research II, Arabian Sea Volume, This issue.

Bauer, S., Hitchcock, G.L., Olson, D.B., 1991. Influence of monsoonally-forced Ekman dynamics upon surface layer depth and plankton biomass distribution in the Arabian Sea. Deep-Sea Research I 38(5), 531–553.

Brink, K., Arnone, R., Coble, P., Flagg, C., Jones, B., Kindle, J., Lee, C., Phinney, D., Wood, M., Yentsch, C., Young, D., 1998. Monsoons Boost Biological Productivity in Arabian Sea. EOS 79(3), 165–169.

Bruce, J.G., Johnson, D.R., Kindle, J.C., 1994. Evidence for eddy formation in the eastern Arabian Sea during the northeast monsoon. Journal of Geophysical Research 99(C4), 7651–7664.

Bruland, K.W., Coale, K.H., 1986. Surface water ^{234}Th/^{238}U disequilibria: spatial and temporal variations of scavenging rates within the Pacific Ocean. In: Burton, J.D., Brewer, P.G., Chesselet, R. (Eds.), Dynamic Processes in the Chemistry of the Upper Ocean, Plenum Press, New York, pp. 159–172.

Buesseler, K.O., 1991. Do upper-ocean sediment traps provide an accurate record of particle flux? Nature 353, 420–423.

Buesseler, K.O., 1998. The de-coupling of production and particulate export in the surface ocean. Global Biogeochemical Cycles 12(2), 297–310.

Buesseler, K.O., Bacon, M.P., Cochran, J.K., Livingston, H.D., 1992a. Carbon and nitrogen export during the JGOFS North Atlantic Bloom Experiment estimated from 234Th:238U disequilibria. Deep-Sea Research I 39(7/8), 1115–1137.

Buesseler, K.O., Cochran, J.K., Bacon, M.P., Livingston, H.D., Casso, S.A., Hirschberg, D., Hartman, M.C., Fleer, A.P., 1992b. Determination of thorium isotopes in seawater by non-destructive and radiochemical procedures. Deep-Sea Research I 39(7/8), 1103–1114.

Buesseler, K., Michaels, A.F., Siegel, D.A., Knap, A.H., 1994. A three dimensional time-dependent approach to calibrating sediment trap fluxes. Global Biogeochemical Cycles 8(2), 179–193.

Buesseler, K.O., Andrews, J.A., Hartman, M.C., Belastock, R., Chai, F., 1995. Regional estimates of the export flux of particulate organic carbon derived from thorium-234 during the JGOFS EQPAC program. Deep-Sea Research Part II 42(2–3), 777–804.

Buesseler, K.O., Ball, L., Andrews, J., Belastock, R., Benitez-Nelson, C., 1996. Upper ocean particulate export in the Arabian Sea. EOS 77 (46), F96.

Burd, A., Moran, S.B., Jackson, G.A., 1998. A coupled adsorption-aggregation model of the POC/^{234}Th ratio of marine particles. Deep-Sea Research, in press.

Chao, Yi., Fu, L.-L., 1995. A comparison between TOPEX/POSEIDON data and a global ocean general circulation model during 1992–1993. Journal of Geophysical Research 100, 965–976.

Charette, M.A., Moran, S.B., 1998. Rates of particle scavenging and particulate organic carbon export estimated using ^{234}Th as a tracer in the subtropical and equatorial Atlantic Ocean. Deep-Sea Research, in press.

Chen, J.H., Edwards, R.L., Wasserburg, G.J., 1986. ^{238}U, ^{234}U and ^{232}Th in seawater. Earth and Planetary Science Letters 80, 241–251.

Coale, K.H., Bruland, K.W., 1987. Oceanic stratified euphotic zone as elucidated by ^{234}Th:^{238}U disequilibria. Limnology and Oceanography 32(1), 189–200.

Cochran, J.K., Barnes. C., Achman, D., Hirschberg, D.J., 1995. Thorium-234/Uranium-238 Disequilibrium as an Indicator of Scavenging Rates and Particulate Organic Carbon Fluxes in the Northeast Water Polynya, Greenland. Journal of Geophysical Research 100(C3), 4399–4410.

Cochran, J.K., Roberts, K.A., Barnes, C., Achman, D., 1997. Radionuclides as indicators of particle and carbon dynamics on the East Greenland Shelf. In: Germain, P., Guary, J.C., Guegueniat, P., Metivier, H. (Eds.), Radioprotection- Colloques, 32 (C2), Proceedings of RADOC 96–97 Radionuclides in the Oceans, pp. 129–136.

Downs, J.N., 1989. Export of Production in Oceanic Systems: information from Phaeopigment, Carbon and Nitrogen Analyses. Ph.D. Thesis, University of Washington.

Eppley, R.W., Peterson, B.J., 1979. Particulate organic matter flux and planktonic new production in the deep ocean. Nature 282, 670–680.

Eppley, R.W., 1989. New production: history, methods, problems. In: Berger, W.H., Smetacek, V.S., Wefer, G. (Eds.), Productivity of the Ocean: Present and Past. Wiley, New York, pp. 85–97.

Flagg, C.N., Kim, H.-S., 1998. Upper ocean currents in the northern Arabian Sea from shipboard ADCP measurements collected during the 1994–1996 JGOFS and ONR Programs. Deep-Sea Research II 45, 1917–1959.

Gallacher, P.C., Rochford, P.A., 1995. Numerical simulations of the Arabian Sea using tracers as proxies for phytoplankton biomass. Journal of Geophysical Research 100(C9), 18 565–18 579.

Gustafsson, Ö., Gschwend, P.M., Buesseler. K.O., 1997. Using ^{234}Th disequilibria to estimate the vertical removal rates of polycyclic aromatic hydrocarbons from the surface ocean. Marine Chemistry 57, 11–23.

Gustafsson, Ö., Buesseler, K.O., Geyer, W.R. Moran. S.B., Gschwend, P.M., 1998. On the relative importance of horizontal and vertical transport of particle-reactive chemicals in the coastal ocean: two-dimensional Th-234 Modeling. Continental Shelf Research 18, 805–829.

Haake, B., Ittekkot, V., Rixen, T., Ramaswamy, V., Nair, R.R., Curry, W.B., 1993. Seasonality and interannual variability of particle fluxes to the deep Arabian Sea. Deep-Sea Research I 40(7), 1323–1344.

Hansell, D.A., Peltzer, E. T., 1998. Spatial and temporal variations of total organic carbon in the Arabian Sea. Deep-Sea Research II 45, 2171–2193.

Hartman, M.C., Buesseler, K.O., 1994. Adsorbers for in-situ collection and at-sea gamma analyses of dissolved Thorium-234 in seawater. WHOI Technical Report 94-15. Woods Hole Oceanographic Institution, Woods Hole, MA U.S.A. 19 pp.

Hellerman, S., Rosenstein, M., 1983. Normal monthly wind stress over the world ocean with error estimates. Journal of Physical Oceanogrophy 13, 1093–1104.

Honjo, S., Dymond, J., Prell, W., Ittekkott, V., 1998. Monsoon-controlled export fluxes to the interior of the Arabian Sea: U.S. JGOFS 1994–1995. Deep-Sea Research II, submitted.

Latasa, M., Bidigare, R.R., 1998. A Comparison of Phytoplankton Populations of the Arabian Sea During the Spring Intermonsoon and Southwest Monsoon of 1995 as Described by HPLC-analyzed Pigments. Deep-Sea Research II 45, 2133–2170.

Lee, C., Murray, D.W., Barber, R.T., Buesseler, K.O., Dymond, J., Hedges, J.I., Honjo, S., Manganini, S.J., Marra, J., Mosers, C., Peterson, M.L., Prell W.L., Wakeham, S.G., 1998. Particulate organic carbon fluxes: results from the U.S. JGOFS Arabian Sea Process Study. Deep-Sea Research II 45, 2489–2501.

Levitus, S., 1982. Climatological atlas of the world ocean. NOAA Prof. paper 13, 173 pp., U.S. Govt. Print. Off., Washington, DC.

Livingston, H.D., Cochran, J.K., 1987. Determination of transuranic and thorium isotopes in ocean water: in solution and filterable particles. Journal of Radioanalysis and Nuclear Chemistry Articles 115, 299–308.

McCreary, J.P. Jr., Kohler, K.E., Hood, R.R., Olson, D.B., 1996. A four-component ecosystem model of biological activity in the Arabian Sea. Progress in Oceanography 37, 193–240.

Measures, C.I., Vink, S., 1998. Seasonal variations in the distribution of Fe and Al in the surface waters of the Arabian Sea. Deep-Sea Research II, in press.

Morrison, J., Codispoti, L.A., Gaurin, S., Jones, B., Manghnani, V., Sheng, Z., 1998. Seasonal variation of the hydrographic and nutrient fields during the US JGOFS Arabian Sea Process Study. Deep-Sea Research II 45, 2053–2101.

Murray, J.W., Downs, J.N., Strom, S., Wei, C.-L., Jannasch, H.W., 1989. Nutrient assimilation, export production and ^{234}Th scavenging in the eastern Equatorial Pacific. Deep-Sea Research 36(10), 1471–1489.

Murray, J.W., Young, J., Newton, J., Dunne, J., Chapin, T., Paul, B., 1996. Export flux of particulate organic carbon from the central Equatorial Pacific determined using a combined drifting trap-^{234}Th approach. Deep-Sea Research II 43, 1095–1132.

Nair, R.R., Ittekkot, V., Manganini, S.J., Ramaswamy, V., Haake, B., Degens, E.T., Desai, B.N., Honjo, S., 1989. Increased particle flux to the deep ocean related to monsoons. Nature 338, 749–751.

Pacanowski, R., Philander, S.G.H., 1981. Parameterization of vertical mixing in numerical models of tropical oceans. Journal of Physical Oceanography 11, 1443–1451.

Pacanowski, R., Dixon, K., Rosati, A., 1991. Modular Ocean Model Users Guide. Ocean Group Tech. Rep. 2, Geophys. Fluid Dyn. Lab., Princeton, NJ.

Ramaswamy, V., Nair, R.R., Manganini, S., Haake, B., Ittekkot, V., 1991. Lithogenic fluxes to the deep Arabian Sea measured by sediment traps. Deep-Sea Research 38(2), 169–184.

Rutgers van der Loeff, M.M., Friedrich, J., Bathmann, U.V., 1996. Carbon export during the spring bloom at the Southern Polar Front, determined with the natural tracer ^{234}Th. Deep-Sea Research II 44(1–2), 457–478.

Sarin, M.M., Krishnaswami, S., Ramesh, R., Somayajulu, B.L.K., 1994. ^{238}U decay series nuclides in the northeastern Arabian Sea: Scavenging rates and cycling processes. Continental Shelf Research 14(2/3), 251–265.

Sarin, M.M., Rengarajan, R., Ramaswamy, V., 1996. ^{234}Th scavenging and particle export fluxes from the upper 100 m of the Arabian Sea. Current Science 71(11), 888–893.

Shimmield, G.B., Ritchie, G.R., 1995. The impact of marginal ice zone processes on the distribution of ^{210}Pb, ^{210}Po and ^{234}Th and implications for new production in the Bellingshausen Sea, Antarctica. Deep-Sea Research II 42(4–5), 1313–1335

Tanaka, N., Takeda, Y., Tsunogai, S., 1983. Biological effect on removal of Th-234, Po-210 and Pb-210 from surface water in Funka Bay, Japan. Geochimica et Cosmochimica Acta 47, 1783–1790.

Wei, C.-L., Murray, J.W., 1992. Temporal variations of ^{234}Th activity in the water column of Dabob Bay: Particle scavenging. Limnology and Oceanography 37(2), 296–314.

Weller, R.A., Baumgartner, M.F., Josey, S.A., Fischer, A.S., Kindle, J., 1998. Atmospheric forcing in the Arabian Sea during 1994–1995: observations and comparisons with climatology and models. Deep-Sea Research II 45, 1961–1999.